

**Manuscript version: Author's Accepted Manuscript**

The version presented in WRAP is the author's accepted manuscript and may differ from the published version or Version of Record.

**Persistent WRAP URL:**

<http://wrap.warwick.ac.uk/110594>

**How to cite:**

Please refer to published version for the most recent bibliographic citation information. If a published version is known of, the repository item page linked to above, will contain details on accessing it.

**Copyright and reuse:**

The Warwick Research Archive Portal (WRAP) makes this work by researchers of the University of Warwick available open access under the following conditions.

Copyright © and all moral rights to the version of the paper presented here belong to the individual author(s) and/or other copyright owners. To the extent reasonable and practicable the material made available in WRAP has been checked for eligibility before being made available.

Copies of full items can be used for personal research or study, educational, or not-for-profit purposes without prior permission or charge. Provided that the authors, title and full bibliographic details are credited, a hyperlink and/or URL is given for the original metadata page and the content is not changed in any way.

**Publisher's statement:**

Please refer to the repository item page, publisher's statement section, for further information.

For more information, please contact the WRAP Team at: [wrap@warwick.ac.uk](mailto:wrap@warwick.ac.uk).

# Photoactivatable Cell-selective Dinuclear Trans Diazo Platinum(IV) Anticancer Prodrugs

Huayun Shi,<sup>†</sup> Isolda Romero-Canelón,<sup>†‡</sup> Monika Hreusova,<sup>‡§</sup> Olga Novakova,<sup>§</sup> V. Venkatesh,<sup>†</sup> Abraha Habtemariam,<sup>†</sup> Guy J. Clarkson,<sup>†</sup> Ji-inn Song,<sup>†</sup> Viktor Brabec,<sup>§</sup> Peter J. Sadler<sup>†\*</sup>

<sup>†</sup> Department of Chemistry, University of Warwick, Coventry, CV4 7AL, UK

<sup>‡</sup> School of Pharmacy, Institute of Clinical Sciences, University of Birmingham, Birmingham, B15 2TT, UK.

<sup>‡</sup> Department of Biophysics, Faculty of Science, Palacky University, 17. listopadu 12, CZ-77146 Olomouc, Czech Republic

<sup>§</sup> Institute of Biophysics, Czech Academy of Sciences, Kralovopolska 135, CZ-61265 Brno, Czech Republic

E-mail: P.J.Sadler@warwick.ac.uk

**KEYWORDS.** Photoactive, dinuclear, anticancer drug.

Supporting Information

**ABSTRACT:** A series of dinuclear octahedral platinum(IV) complexes *trans*, *trans*, *trans*-[Pt(N<sub>3</sub>)<sub>2</sub>(py)<sub>2</sub>(OH)-(OC(O)CH<sub>2</sub>CH<sub>2</sub>C(O)NH)<sub>2</sub>R] containing pyridine (py) and bridging dicarboxylate (R = -CH<sub>2</sub>CH<sub>2</sub>- (**1**); *trans*-1,2-C<sub>6</sub>H<sub>10</sub>- (**2**); p-C<sub>6</sub>H<sub>4</sub>- (**3**); -CH<sub>2</sub>CH<sub>2</sub>CH<sub>2</sub>CH<sub>2</sub>- (**4**)) ligands have been synthesized and characterized, including the x-ray crystal structures of complexes **1**·2MeOH and **4**, the first photoactivatable dinuclear platinum(IV) complexes with azido ligands. The complexes are highly stable in the dark, but upon photoactivation with blue light (420 nm) they release the bridging ligand and mononuclear photoproducts. On irradiation with blue light (465 nm) they generate azidyl and hydroxyl radicals, detected using a DMPO EPR spin-trap, accompanied by the disappearance of the LMCT (N<sub>3</sub>→Pt) band at *ca.* 300 nm. The dinuclear complexes are photocytotoxic to human cancer cells (465 nm, 4.8 mW/cm<sup>2</sup>, 1 h), including A2780 human ovarian and oesophageal OE19 cells with IC<sub>50</sub> values of 8.8–78.3 μM, whereas cisplatin is inactive under these conditions. Complexes **1**, **3** and **4** are notably more photoactive towards cisplatin-resistant ovarian A2780cis compared to A2780 cells. Remarkably, all the complexes were relatively non-toxic toward normal cells (MRC5 lung fibroblasts), with IC<sub>50</sub> values >100 μM, even after irradiation. The introduction of the aromatic bridging ligand (**3**) enhanced cellular uptake significantly. The populations in the stages of the cell cycle remained unchanged on treatment with complexes in the dark, while the population of the G2/M phase increased on irradiation, suggesting that DNA is a target for these photoactivated dinuclear platinum(IV) complexes. LC-MS data show that the photodecomposition pathway of the dinuclear complexes results in the release of two molecules of mononuclear platinum(II) species. As a consequence, DNA binding of the dinuclear complexes after photoactivation in cell-free media is, in several respects, qualitatively similar to that of the photoactivated mononuclear complex **FM-190**. After photoactivation, they were two-fold more effective in quenching fluorescence of EtBr bound to DNA, forming DNA interstrand cross-links and unwinding DNA compared to photoactivated **FM-190**.

## INTRODUCTION

Photoactivation is a promising effective and non-invasive chemotherapeutic strategy.<sup>1-4</sup> Photochemotherapy using appropriate platinum complexes has the potential to overcome some of the limitations of conventional cisplatin therapy, including poor pharmacokinetics, dose-limiting side effects, restricted spectrum of anticancer activity, high incidence of resistance, and lack of normal-cell discrimination.<sup>5,6</sup> The application of oxygen-dependent photodynamic therapy (PDT) is limited owing to the low concentration of O<sub>2</sub> in hypoxic tumours, together with the need for diffusion of O<sub>2</sub> from adjacent tissues.<sup>7</sup> Photoactivated chemotherapy (PACT), in contrast, is less dependent on oxygen for cytotoxicity and provides a new avenue to anticancer drug design.

Octahedral, low-spin 5d<sup>6</sup> Pt<sup>IV</sup> complexes are usually considered to be prodrugs, since they are kinetically more inert than their Pt<sup>II</sup> counterparts under biological conditions.<sup>8-10</sup> Photoactivatable Pt<sup>IV</sup> prodrugs can exhibit high dark stability and potential photocytotoxicity,<sup>11-13</sup> examples include diazido- Pt<sup>IV</sup> complexes containing various non-leaving amines and axial substituents.<sup>14-20</sup> Among them, *trans*, *trans*, *trans*-[Pt(N<sub>3</sub>)<sub>2</sub>(OH)(py)<sub>2</sub>] (**FM-190**) is highly potent,<sup>21,22</sup> has good aqueous solubility, is relatively stable in cell culture media and towards reactions with the abundant intracellular tripeptide glutathione (GSH, γ-L-Glu-L-Cys-Gly), and can be activated by UVA, blue (420 nm) and green (500±30 nm) light, achieving low micromolar IC<sub>50</sub> values even in cisplatin-resistant cell lines, with a high phototoxicity index. Not only does the platinum center become reactive on photoreduction, but in addition azidyl radicals can be released by **FM-190** in a manner controllable by the amino acid L-Trp.<sup>23</sup>

Axial ligands in diazido-Pt<sup>IV</sup> complexes normally act as leaving groups upon reduction to Pt<sup>II</sup> and greatly influence the reduction potential of Pt<sup>IV</sup>. Derivatisation of an axial ligand can be used to improve pharmacological properties without interfering with the ultimate mode of action of the active Pt<sup>II</sup> species or the potential production of other reactive species. Several studies have been carried out previously on the conjugation of **FM-190** to functional fragments, including α<sub>v</sub>β<sub>3</sub> and α<sub>v</sub>β<sub>5</sub> integrin-selective RGD-

containing peptides,<sup>24</sup> RNA-binding guanidinoneomycin,<sup>25</sup> TEMPO radical<sup>26</sup>, upconversion-luminescent nanoparticles<sup>27</sup> and G-quadruplex G4K<sup>+</sup> borate hydrogels.<sup>28</sup> For the former two conjugates, the selectivity and cellular uptake toward specific cancer cells was remarkably enhanced, while for the prodrug with TEMPO, azidyl and TEMPO radicals were released upon irradiation with blue light (420 nm), accompanied by the formation of toxic Pt<sup>II</sup> species, resulting in improved cytotoxicity. Upconversion-luminescent nanoparticles enable photoactivation with near-infrared light, and hydrogels allow treatment of surface cancers with minimal damage to normal tissues.

Polynuclear platinum complexes have attracted much attention owing to their unique biological properties, including coordinative binding to DNA bases and interaction of the phosphodiester linker through electrostatic and hydrogen-bonding effects.<sup>29</sup> The pre-association of polynuclear platinum complexes with DNA prior to coordinate bond formation can significantly affect the kinetics of cross-link formation,<sup>30-33</sup> which distinguishes them from their mononuclear counterparts. The trinuclear complex  $[\{trans\text{-PtCl}(\text{NH}_3)_2\}_2(\mu\text{-trans-Pt}(\text{NH}_3)_2\{\text{NH}_2(\text{CH}_2)_6\text{NH}_2\})]^{4+}$  (BBR3464) underwent phase I and II human clinical trials as a promising anticancer platinum drug.<sup>34-36</sup>

In order to investigate structure-activity relationships related to the modification of the axial ligands of diazido-Pt<sup>IV</sup> complexes and improve the antiproliferative activity of photoactivatable Pt<sup>IV</sup> prodrugs, we have synthesized and characterized a series of dinuclear platinum(IV) complexes of the type *trans, trans, trans*- $[\{\text{Pt}(\text{N}_3)_2(\text{py})_2(\text{OH})(\text{OC}(\text{O})\text{CH}_2\text{CH}_2\text{C}(\text{O})\text{NH})\}_2\text{R}]$  (R = -CH<sub>2</sub>CH<sub>2</sub>- (**1**); *trans*-1,2-C<sub>6</sub>H<sub>10</sub>- (**2**); *p*-C<sub>6</sub>H<sub>4</sub>- (**3**); -CH<sub>2</sub>CH<sub>2</sub>CH<sub>2</sub>CH<sub>2</sub>- (**4**)). The x-ray crystal structures of complexes **1**·2MeOH and **4** were determined. These appear to be the first photoactivatable dinuclear platinum(IV) complexes containing azides to be reported. Their photodecomposition, photoreactions with 5'-guanosine monophosphate (5'-GMP), interaction with DNA, photocytotoxicity, cellular accumulation, and effect on cancer cell cycle distribution were studied. The chemical and biological behaviour of these complexes containing two platinum centers and four azides in one molecule are compared to related mononuclear diazido complexes, including the influence of the nature of the bridging ligand.

## EXPERIMENTAL SECTION

**Materials and instruments.** O-(Benzotriazol-1-yl)-*N, N, N'*, *N'*-tetramethyluronium tetrafluoroborate (TBTU) was purchased from Merck, Pyridine was from Fischer Scientific UK, *ct*-DNA, K<sub>2</sub>PtCl<sub>4</sub>, NaN<sub>3</sub>, H<sub>2</sub>O<sub>2</sub> (30%), succinic anhydride and other chemicals were from Sigma Aldrich and used without further purification.

NMR spectra were recorded on Bruker Avance III HD 400 MHz or Bruker 500 MHz spectrometers; the residual signal of the solvent was used as a reference. ESI-MS spectra were recorded on an Agilent 6130B single quadrupole detector instrument and ESI-HR-MS data were collected on a Bruker microTOF instrument at 298 K with a scan range of *m/z* 50-2000 for positive ions. Samples were prepared in methanol or aqueous solution. Electronic absorption spectra were recorded on a Varian Cary 300 UV-vis spectrophotometer in a quartz cuvette and referenced to neat solvent. The spectral width was 200–800 nm and the bandwidth was 1.0 nm, the scan rate was set to 600 nm/min. Analytical reversed-phase HPLC analyses were carried out on an Agilent ZORBAX Eclipse XDB-C18 column (250×4.6 mm, 5 μm, flow rate: 1 mL/min), by using linear gradients of 0.1% TFA in H<sub>2</sub>O (solvent A) and 0.1% TFA in CH<sub>3</sub>CN (solvent B). LC-MS were carried out on Bruker Amazon X connected online with a HPLC. The light sources used for photoactivation were a LZC-ICH2 photoreactor (Luzchem Research Inc.) equipped with a temperature

controller and 8 Luzchem LZC-420 lamps without light filtration, and KiloArcTM broadband arc lamp monochromator supplied with the appropriate filters to cut off any unwanted light. An LED light source with λ<sub>max</sub> = 465 nm was used for *in vitro* growth inhibition and cell cycle assays. Platinum contents were analysed on an ICP-OES 5300DV (Perkin Elmer) or ICP-MS 7500cx (Agilent). The emission wavelengths detected for Pt were 265.945, 214.423, 299.797, 204.937 and 193.700 nm.

**Synthesis and characterization.** *Caution!* Heavy metal azides can be shock-sensitive detonators. We did not encounter any problems during the work reported here, but due care and attention with appropriate precautions should be taken in their synthesis and handling. All synthesis and purifications were carried out in the dark with minimal light exposure.

General synthesis procedure for complexes **1–4**. To a solution of *trans, trans, trans*- $[\text{Pt}(\text{N}_3)_2(\text{OH})(\text{succinate})(\text{py})_2]$  (24.4 mg, 42.8 μmol) and TBTU (11.8 mg, 36.8 μmol) in freshly degassed anhydrous DMF (2 mL), *N, N*-diisopropylethylamine (DIPEA) (100 μL) was added. After stirring for 3 min, a solution of 0.5 mol equiv of corresponding diamine, DIPEA (60 μL) and DMF (1 mL) was added to the resulting mixture dropwise. The reaction mixture was stirred overnight at 298 K under a nitrogen atmosphere. After evaporation to dryness, the oily residue was collected and purified by column chromatography on aluminium oxide (5% methanol + 95% DCM).

*Trans, trans, trans*- $[\{\text{Pt}(\text{N}_3)_2(\text{py})_2(\text{OH})(\text{OC}(\text{O})\text{CH}_2\text{CH}_2\text{C}(\text{O})\text{NH})\}_2(\text{CH}_2)_2]$  (**1**). Diamine = ethylenediamine. <sup>1</sup>H NMR (DMSO-*d*<sub>6</sub>, 400 MHz): 8.81(dd, *J* = 5.5 Hz, *J*<sup>195Pt-H</sup> = 26.6 Hz, 8H, *H<sub>α</sub>* py), 8.26 (t, *J* = 7.5 Hz, 4H, *H<sub>γ</sub>* py), 7.82 (t, *J* = 7.0 Hz, 8H, *H<sub>β</sub>* py), 7.75 (t, *J* = 5.7 Hz, 2H, *CONH*), 3.66 (s, 2H, *OH*), 3.05 (s, 4H, *CH*<sub>2</sub>), 2.46 (t, *J* = 7.6 Hz, 4H, *CH*<sub>2</sub>), 2.22 (t, *J* = 7.3 Hz, 4H, *CH*<sub>2</sub>). <sup>13</sup>C NMR (DMSO-*d*<sub>6</sub>, 125 MHz): 175.27 (*COO*), 172.08 (*CONH*), 149.83 (*C<sub>α</sub>* py), 142.42 (*C<sub>γ</sub>* py), 126.66 (*C<sub>β</sub>* py), 38.80 (*CH*<sub>2</sub>), 32.39 (*CH*<sub>2</sub>), 32.21 (*CH*<sub>2</sub>). ESI-MS [*M*+*Na*<sup>+</sup>]: 1189.2160. Anal. Calcd: C<sub>30</sub>H<sub>36</sub>N<sub>18</sub>O<sub>8</sub>Pt<sub>2</sub>: C 30.88, H 3.11, N 21.61. Found: C 30.43, H 3.10, N 20.69.

*Trans, trans, trans*- $[\{\text{Pt}(\text{N}_3)_2(\text{py})_2(\text{OH})(\text{OC}(\text{O})\text{CH}_2\text{CH}_2\text{C}(\text{O})\text{NH})\}_2(\text{trans-1,2-C}_6\text{H}_{10})]$  (**2**). Diamine = *trans*-1,2-cyclohexanediamine. <sup>1</sup>H NMR (DMSO-*d*<sub>6</sub>, 400 MHz): 8.82(dd, *J* = 5.5 Hz, *J*<sup>195Pt-H</sup> = 26.5 Hz, 8H, *H<sub>α</sub>* py), 8.25 (t, *J* = 7.5 Hz, 4H, *H<sub>γ</sub>* py), 7.82 (t, *J* = 6.9 Hz, 8H, *H<sub>β</sub>* py), 7.52 (d, *J* = 7.3 Hz, 2H, *CONH*), 3.66 (s, 2H, *OH*), 3.47 (s, 2H, *CH*<sub>2</sub> cyclohexyl), 2.48-2.33 (m, 4H, *CH*<sub>2</sub>), 2.26-2.10 (m, 4H, *CH*<sub>2</sub>), 1.74 (s, 2H, *CH*<sub>2</sub> cyclohexyl), 1.62 (s, 2H, *CH*<sub>2</sub> cyclohexyl), 1.18 (s, 4H, *CH*<sub>2</sub> cyclohexyl). <sup>13</sup>C NMR (DMSO-*d*<sub>6</sub>, 125 MHz): 175.23 (*COO*), 171.68 (*CONH*), 149.84 (*C<sub>α</sub>* py), 142.38 (*C<sub>γ</sub>* py), 126.65 (*C<sub>β</sub>* py), 55.38 (*CH*<sub>2</sub> cyclohexyl), 52.50 (*CH* cyclohexyl), 49.06 (*CH* cyclohexyl), 32.74 (*CH*<sub>2</sub>), 32.58 (*CH*<sub>2</sub>), 32.10 (*CH*<sub>2</sub> cyclohexyl), 24.87 (*CH*<sub>2</sub> cyclohexyl). ESI-MS [*M*+*Na*<sup>+</sup>]: 1243.2631. Anal. Calcd: C<sub>34</sub>H<sub>42</sub>N<sub>18</sub>O<sub>8</sub>Pt<sub>2</sub>: C 33.45, H 3.47, N 20.65. Found: C 33.84, H 3.48, N 19.14.

*Trans, trans, trans*- $[\{\text{Pt}(\text{N}_3)_2(\text{py})_2(\text{OH})(\text{OC}(\text{O})\text{CH}_2\text{CH}_2\text{C}(\text{O})\text{NH})\}_2(1,4\text{-C}_6\text{H}_4)]$  (**3**). Diamine = *p*-phenylenediamine. <sup>1</sup>H NMR (DMSO-*d*<sub>6</sub>, 400 MHz): 9.79 (s, 2H, *CONH*), 8.82(dd, *J* = 5.5 Hz, *J*<sup>195Pt-H</sup> = 26.7 Hz, 8H, *H<sub>α</sub>* py), 8.25 (t, *J* = 7.3 Hz, 4H, *H<sub>γ</sub>* py), 7.79 (t, *J* = 7.1 Hz, 8H, *H<sub>β</sub>* py), 7.50 (s, 4H, *CH* benzyl), 3.67 (s, 2H, *OH*), 2.67 (t, *J* = 7.3 Hz, 4H, *CH*<sub>2</sub>), 2.33 (t, *J* = 7.6 Hz, 4H, *CH*<sub>2</sub>). <sup>13</sup>C NMR (DMSO-*d*<sub>6</sub>, 125 MHz): 175.20 (*COO*), 170.71 (*CONH*), 149.83 (*C<sub>α</sub>* py), 142.39 (*C<sub>γ</sub>* py), 135.10 (*C* benzyl), 126.64 (*C<sub>β</sub>* py), 119.77 (*CH* benzyl), 33.09 (*CH*<sub>2</sub>), 32.13 (*CH*<sub>2</sub>). ESI-MS [*M*+*Na*<sup>+</sup>]: 1237.2138. Anal. Calcd: C<sub>34</sub>H<sub>36</sub>N<sub>18</sub>O<sub>8</sub>Pt<sub>2</sub>·Et<sub>2</sub>O: C, 35.41; H, 3.60; N, 19.56. Found: C, 35.54; H, 3.76; N, 19.96.

*Trans, trans, trans*- $[\{\text{Pt}(\text{N}_3)_2(\text{py})_2(\text{OH})(\text{OC}(\text{O})\text{CH}_2\text{CH}_2\text{C}(\text{O})\text{NH})\}_2(\text{CH}_2)_4]$  (**4**). Diamine = 1,4-butylenediamine. <sup>1</sup>H NMR (DMSO-*d*<sub>6</sub>, 400 MHz): 8.82(dd, *J* = 5.5 Hz, *J*<sup>195Pt-H</sup> = 26.9 Hz,

8H,  $H_{\alpha}$  py), 8.27 (t,  $J = 7.6$  Hz, 4H,  $H_{\gamma}$  py), 7.83 (t,  $J = 7.0$  Hz, 8H,  $H_{\beta}$  py), 7.71 (t,  $J = 5.5$  Hz, 2H, CONH), 3.65 (s, 2H, OH), 3.00 (m, 4H,  $CH_2$ ), 2.45 (t,  $J = 7.3$  Hz, 4H,  $CH_2$ ), 2.23 (t,  $J = 7.4$  Hz, 4H,  $CH_2$ ), 1.34 (s, 4H,  $CH_2$ ).  $^{13}C$  NMR (DMSO- $d_6$ , 125 MHz): 175.28 (COO), 171.72 (CONH), 149.84 ( $C_{\alpha}$  py), 142.41 ( $C_{\gamma}$  py), 126.66 ( $C_{\beta}$  py), 38.69 ( $CH_2$ ), 32.51 ( $CH_2$ ), 32.21 ( $CH_2$ ), 27.10 ( $CH_2$ ). ESI-MS [ $M+Na^+$ ]: 1217.2461. Anal. Calcd:  $C_{32}H_{40}N_{18}O_8Pt_2$ : C 32.16, H 3.37, N 21.10. Found: C 32.44, H 3.36, N 20.30.

**X-Ray crystallography.** Single crystals of **1**·2MeOH and **4** were grown from methanol/ether at ambient temperature. A suitable crystal was selected and mounted on a Mitegen head with Fomblin oil and placed on an Xcalibur Gemini diffractometer with a Ruby CCD area detector. The crystal was kept at 150(2) K during data collection. Using Olex2,<sup>37</sup> the structure was solved with the ShelXT<sup>38</sup> structure solution program using Intrinsic Phasing and refined with the ShelXL<sup>39</sup> refinement package using Least Squares minimisation.

**Photodecomposition in solution.** The photodecomposition of complexes **1–4** in aqueous solution was monitored by UV-Vis spectroscopy or LC-MS at different time intervals after irradiation with blue light (420 nm) at ambient temperature.

**Cell culture.** A number of human cell lines, parental (A2780) and cisplatin resistant (A2780cis) ovarian carcinoma, oesophageal adenocarcinoma (OE19), and normal fibroblasts cells (MRC5) were obtained from the European Collection of Animal Cell Culture (ECACC), Salisbury, UK. All cell lines used in this work were grown in Roswell Park Memorial Institute media (RPMI-1640), which was supplemented with 10% v/v of foetal calf serum (FCS), 1% v/v of 2 mM glutamine and 1% v/v penicillin/streptomycin. The adherent monolayers of cells were grown at 310 K in a humidified atmosphere containing 5% CO<sub>2</sub> and passaged regularly at ca. 80% confluence.

**Photo-dark cytotoxicity.** Approximately 10000 cells were seeded per well in 96-well plates. Independent duplicate plates were used, one for dark while the other for irradiation experiment. The cells were pre-incubated in drug-free media with phenol red containing medium at 310 K for 24 h before adding different concentrations of the compounds to be tested prepared in phenol-free medium. Complexes were dissolved first in DMSO and then diluted in phenol red-free RPMI-1640 to make the stock solution of the drug. These stock solutions were further diluted using phenol-red free cell culture medium until working concentrations were achieved, in these solutions the maximum DMSO concentration was in all cases < 0.5% v/v. Cells were exposed to the drugs with different concentrations for 1 h. Then one plate was irradiated for 1 h using blue light (4.8 mW cm<sup>-2</sup> per LED at 465 nm) while the dark plate was kept in the incubator. After irradiation, supernatants of both plates were removed by suction and washed with PBS buffer. Photocytotoxicity was determined after another 24 h recovery at 310 K in drug-free phenol red-containing medium by comparison to untreated controls which were only exposed to vehicle. Untreated controls were also compared between the irradiated and the non-irradiated plates to ensure that the differences in cell survival were not statistically relevant, hence guaranteeing that the differences in cell viability observed were not due to the light source. The SRB assay was used to determine cell viability.<sup>40</sup> Absorbance measurements of the solubilised dye (on a Promega microplate reader, 510 nm) allowed the determination of viable treated cells compared to untreated controls. IC<sub>50</sub> values (concentrations which caused 50% of cell death), were determined as the average of triplicates and their standard deviations were calculated. Stock concentrations for all metal complexes used in these biological assays were adjusted/verified after ICP-OES metal quantification.

**Platinum accumulation in cancer cells.** For Pt cellular accumulation studies, ca.  $4.5 \times 10^6$  A2780, A2780cis and OE19 cells were plated in 100 mm Petri dishes and allowed to attach for 24 h. Then the plates were exposed to complexes at equipotent concentrations equal to the photoactive IC<sub>50</sub> values in the corresponding cell line. Additional plates were incubated with medium alone as a negative control. After 1 h of incubation in the dark at 310 K, the cells were rinsed three times with cold phosphate-buffered saline (PBS) and harvested by trypsinisation. The number of cells in each sample was counted manually using a haemocytometer. Then the cells were centrifuged to obtain the whole cell pellet for ICP-MS analysis. All experiments were conducted in triplicate.

**ICP-MS sample preparation.** The whole cell pellets were dissolved in concentrated 72% v/v nitric acid (200  $\mu$ L), and the samples were then transferred into wheaton v-vials (Sigma-Aldrich) and heated in an oven at 343 K overnight. The vials were then allowed to cool, and each cellular sample solution was transferred into a vial and diluted with Milli-Q water (3.8 mL), to obtain a final HNO<sub>3</sub> concentration of ca. 3.6% v/v.

**Photoreactions with 5'-GMP.** 2, 4 or 8 mol equiv of guanosine 5'-monophosphate disodium salt hydrate (5'-GMP-Na<sub>2</sub>) was mixed with 30  $\mu$ M complex **4** in methanol:water 5:95 v/v. The solution was incubated at 310 K for 1 h then irradiated for 1 h and analysed immediately. HPLC analysis was carried out on an Agilent ZORBAX Eclipse XDB-C18 column (250  $\times$  4.6 mm, 5  $\mu$ m, flow rate: 1 mL/min). The mobile phases for HPLC were A (0.1 % formic acid in HPLC grade H<sub>2</sub>O, volume percentage) and B (0.1 % formic acid in HPLC grade acetonitrile, volume percentage). The Pt adducts were isolated and analysed by Bruker Amazon X connected online with the HPLC.

**Electron paramagnetic resonance (EPR) spectroscopy.** The EPR spectra were recorded on a Bruker EMX (X-band) spectrometer at 298 K. Samples (ca. 100  $\mu$ L) in aqueous solution were prepared and transferred using a plastic syringe with metal needle to a standard quality quartz tube with inner diameter of 1.0 mm and outer diameter of 2.0 mm (Wilma LabGlass) and sealed with parafilm. Using the y-incremental sweep mode of 120 with an accumulation of 5 scans in the x dimension, Typical key EPR spectrometer settings were modulation amplitude 2.0 G, microwave power 1.37 mW,  $1.0 \times 10^5$  receiver gain, conversion time 5.12 ms, time constant 5.12 ms, sweep width 200 G. The LED465E light irradiation source was mounted within the EPR magnet, supported by a foam sponge, to maintain its position throughout the EPR measurements. The distance from the tip of the irradiation light bulb to the EPR cavity was ca. 3 cm. Data were processed by Matlab R2016b with easyspin 5.1.12 through a multicomponent fit.

**Flow cytometry.** All flow cytometry experiments were carried out using a Becton Dickinson FACScan Flow Cytometer in the School of Life Sciences at Warwick University. Typically, cells were seeded in 6-well plates using  $1.5 \times 10^6$  cells per well. Experiments included 24 h of pre-incubation in drug-free media at 310 K in CO<sub>2</sub> humidified atmosphere, followed by 1 h of drug exposure under the same conditions. After this, samples were irradiated for 1 h. For comparison, the dark plates were kept in the incubator for another 1 h. Supernatants were removed, cells were washed with PBS. Samples were then collected after trypsinization, washed with PBS and stained in the dark with a mixture of propidium iodide and RNase. After 30 min staining, cell samples were washed and set up for flow cytometry reading on the red channel FL-2.

**Kinetics of binding to ct-DNA.** ct-DNA was mixed with complexes in 10 mM NaClO<sub>4</sub> and immediately irradiated (visible light,  $\lambda_{max} = 455$  nm) for 60 or 120 min and then kept at 310 K in

the dark. The  $r_i$  value was 0.05-0.08. Aliquots were removed at various time intervals and quickly filtered using a Sephadex G-50 column to remove free (unbound) Pt. The Pt content in these DNA samples ( $r_b$ , defined as the number of the molecules of platinum complex coordinated per nucleotide residue) was determined by AAS and concentration of DNA by UV-vis spectroscopy.

**Characterization of DNA Adducts of Photoactivated complexes by EtBr Fluorescence.** *ct*-DNA was incubated with the Pt complexes under irradiation conditions (visible light,  $\lambda_{\max} = 455$  nm for 2 h and subsequently incubated in the dark for an additional 23 h) at various  $r_b$  values in 10 mM NaClO<sub>4</sub> at 310 K. Fluorescence measurements of *ct*-DNA modified by Pt complexes in the presence of EtBr were performed at an excitation wavelength of 546 nm, and the emitted fluorescence was analyzed at 590 nm. The fluorescence intensity was measured in NaCl (0.4 M) to avoid secondary binding of EtBr to DNA. The concentrations were 0.01 mg mL<sup>-1</sup> for DNA and 0.04 mg mL<sup>-1</sup> for EtBr, which corresponded to the saturation of all binding sites for EtBr in DNA. The fluorescence spectra were recorded by a Varian Cary Eclipse spectrofluorophotometer using a 0.5 cm quartz cell at room temperature.

**Formation of interstrand cross-links.** Solutions of the plasmid pUC19 linearized by EcoRI (50  $\mu$ g mL<sup>-1</sup>) were incubated with the Pt complex under irradiation conditions (for 1 h and subsequently incubated in the dark for an additional 23 h) at various  $r_i$  values in NaClO<sub>4</sub> (10 mM) at 310 K. Autoradiograms were recorded of denaturing 1% agarose gel of linearized DNA which was 3'-end labeled and nonmodified or modified by **FM-190**, **1** and **4** photoactivated by visible light.

**Transcription mapping of platinum-DNA adducts.** Transcription of the (NdeI/HpaI) restriction fragment of pSP73KB DNA modified by cisplatin, transplatin or **1**, **4** and **FM-190** in the dark or photoactivated by visible light ( $\lambda_{\max} = 455$  nm for 1 h and subsequently incubated 23 h in the dark, 310 K, 10 mM NaClO<sub>4</sub>) with DNA-dependent T7 RNA polymerase and electrophoretic analysis of transcripts was performed according to the protocols recommended by the manufacturer (Promega Protocols and Applications, 43-46, 1989/90) and described in detail previously.<sup>19</sup> The concentration of DNA in this assay was  $1.54 \times 10^{-4}$  M (relative to the monomeric nucleotide content). The  $r_i$  values for platination reactions were chosen so as to obtain an  $r_b$  value in the range 0.001 - 0.01. Pt complexes not bound to DNA were removed by ethanol precipitation.

**Unwinding of Negatively Supercoiled DNA.** Negatively supercoiled pSP73KB plasmid was treated with **FM-190**, **1** or **4** photoactivated by visible light ( $\lambda = 420$  nm) for 1 h and incubated for 23 h at 310 K in the dark. The degree of supercoiling was monitored using electrophoresis in 1% native agarose gel. The unwinding angle is given by  $\Phi = -18\sigma/r_b(c)$ , where  $\sigma$  is the superhelical density (-0.063), and  $r_b(c)$  is the value of  $r_b$  at which the supercoiled and nicked forms comigrate.

**DNase I Footprinting.** Supercoiled pSP73 plasmid was digested with Hind III restriction endonuclease and 3'-end-labeled by treatment with Klenow *exo-* and [ $\alpha$ -<sup>32</sup>P]-deoxy-ATP. After radioactive labelling, the DNA first cleaved with Hind III was further digested with Nde I to yield 158 and 2306 bp fragments. The 158 bp fragment was purified by 1% agarose gel electrophoresis and isolated from the gel by a Promega Wizard SV Gel cleanup system.

Radioactively labelled DNA ( $5.4 \times 10^{-6}$  M) and the Pt complex ( $r_i = 0.1, 0.2, 0.4$ ) in 10 mM NaClO<sub>4</sub> was irradiated by  $\lambda = 420$  nm for 1 h and incubated for 23 h at 310 K in the dark. Radioactively labelled DNA and the Pt complex at  $r_i = 0.4$  were also incubated in the dark for 24 h at 310 K. The reaction mixture was then lyophilized and dissolved in 9  $\mu$ L solution containing a  $1.11 \times$

TKMC buffer (10 mM Tris, pH 7.9, 10 mM KCl, 10 mM MgCl<sub>2</sub>, and 5 mM CaCl<sub>2</sub>) and 3  $\mu$ g *ct*-DNA. Cleavage was initiated by the addition of 0.25 U of DNase I (one unit of RQ1 RNase-Free DNase is defined as the amount required to completely degrade 1  $\mu$ g of lambda DNA in 10 min at 310 K in 50  $\mu$ L of a buffer containing 40 mM Tris-HCl (pH 7.9), 10 mM NaCl, 6 mM MgCl<sub>2</sub> and 10 mM CaCl<sub>2</sub>) and allowed to react for 30 s at 298 K before quenching with 2.5  $\mu$ L of a DNase stop solution (3 M NaOAc and 0.25 M EDTA). This was then precipitated with ethanol, lyophilized, and resuspended in a formamide loading buffer. DNA cleavage products were resolved by poly(acrylamide) (PAA) gel electrophoresis under denaturing conditions (8%/8 M urea PAA gel). The autoradiograms were visualized and quantified by using a bioimaging analyzer. Assignment of the cleavage to a particular base has been made so that it corresponds to cleavage of the phosphodiesteric bond on the 5' side of that base.

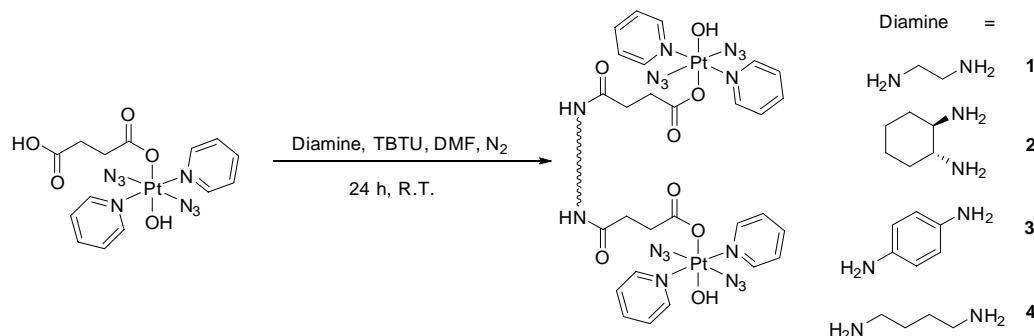
## RESULTS AND DISCUSSION

**Synthesis and characterization of complexes 1-4.** The synthetic route for dinuclear Pt<sup>IV</sup> complexes **1-4** is summarized in Scheme 1. The mononuclear complexes *trans*, *trans*, *trans*-[Pt(N<sub>3</sub>)<sub>2</sub>(OH)<sub>2</sub>(py)<sub>2</sub>] (**FM-190**) and *trans*, *trans*, *trans*-[Pt(N<sub>3</sub>)<sub>2</sub>(OH)(OC(O)CH<sub>2</sub>CH<sub>2</sub>C(O)OH)(py)<sub>2</sub>] (**FMSA**) were prepared by similar procedures to those reported.<sup>26</sup> The two Pt<sup>IV</sup> centers with axial succinate carboxylates were coupled through amide bond formation using bridging diamines containing ethylene (**1**), 1,2-cyclohexyl (**2**), 1,4-phenylene (**3**), or butyl (**4**) linkers. Complexes **1-4** are air-stable at ambient temperature, both in the solid state and in aqueous solution. They gave satisfactory elemental analysis and were further characterized by ESI-MS, NMR and UV/Vis spectroscopy, and for complexes **1** and **4** by x-ray crystallography.

The <sup>1</sup>H and <sup>13</sup>C NMR spectra of complexes **1-4** in DMSO-*d*<sub>6</sub> contain the expected peaks (Figures S1-S8). In the <sup>1</sup>H NMR spectra, the doublets with <sup>195</sup>Pt satellites at *ca.* 8.82 ppm ( $J = 5.5$  Hz,  $J^{195\text{Pt-H}} = 26.6$  Hz) and the triplets at *ca.* 8.26 ppm ( $J = 7.5$  Hz), 7.82 ppm ( $J = 7.0$  Hz) are assigned to the *Ha*, *Hy* and *H $\beta$*  of pyridine, respectively. The peaks at *ca.* 3.66 ppm are assignable to the resonances of the hydroxyl protons and the peaks at 7.52-9.79 ppm to the amide protons. The <sup>13</sup>C NMR resonances of complexes **1-4** at *ca.* 149.83, 142.40 and 126.66 ppm are attributable to the *Ca*, *C $\gamma$*  and *C $\beta$*  carbons of pyridine, respectively. The complexes all display peaks at *ca.* 175.27 and 172.00 ppm for the carboxyl and amide carbons, respectively. The electronic absorption spectrum of complex **1** is similar to that of its mononuclear analogue *trans*, *trans*, *trans*-[Pt(N<sub>3</sub>)<sub>2</sub>(OH)<sub>2</sub>(py)<sub>2</sub>]. In water/methanol (2:3) solution, complex **1** shows a high-energy band at 262 nm ( $\epsilon = 25260$  M<sup>-1</sup>cm<sup>-1</sup>) and a maximum absorption band at 300 nm (34109 M<sup>-1</sup>cm<sup>-1</sup>), which are assigned to a LMCT (OH $\rightarrow$ Pt, N<sub>3</sub> $\rightarrow$ Pt) transition. In addition, a weak band is observed at 420 nm that has mixed <sup>1</sup>LMCT/<sup>1</sup>IL character and involves N<sub>3</sub> and OH ligands and platinum.<sup>21</sup> This band enables the photoactivation of complex **1** using blue light. Complexes **2-4** show similar electronic absorption spectra as complex **1**, except that the high-energy band (at 260 nm,  $\epsilon = 49189$  M<sup>-1</sup>cm<sup>-1</sup>) of complex **3** is more intense than those of its analogues ( $\epsilon \approx 25000$  M<sup>-1</sup>cm<sup>-1</sup>), owing to the absorption of the phenyl fragment.

**X-ray crystallography.** Crystals suitable for X-ray diffraction studies of complexes **1**·2MeOH and **4** were obtained through the diffusion of diethyl ether into corresponding solutions in methanol. The structure of complexes **1**·2MeOH and **4** are shown in Figure 1. The crystallographic data are summarized in Table S1 and selected bond distances and angles are listed in Table 1. Complex **1**·2MeOH crystallized in the triclinic space group P-1 with one complex and two methanol molecules in the unit cell. Complex **4** crystallized in

**Scheme 1.** The synthetic route for photoactive dinuclear diazido platinum(IV) complexes **1–4**.



the monoclinic space group  $P2_1/n$  with two molecules in the unit cell.

Complexes **1**·MeOH and **4** are neutral and consist of two mononuclear  $Pt^{IV}$  fragments bridged by an aliphatic linker of a diamine which forms amide bonds to the axial succinate carboxylates. The two Pt centers are symmetric with the diamine linker sitting on an inversion center. The geometries of the Pt centers are similar to their mononuclear analogue *trans, trans, trans*-[Pt(N<sub>3</sub>)<sub>2</sub>(OH)<sub>2</sub>(py)<sub>2</sub>]: octahedral with [N<sub>4</sub>O<sub>2</sub>] coordination. The equatorial plane is defined by four nitrogen atoms, two from the *trans* pyridine molecules and two from the *trans* azides. An oxygen atom from a hydroxido ligand is located in an axial position, while the other axial position is occupied by an oxygen from one of the succinate carboxylate groups.

(2.053(2) and 2.052(2) Å). The amide C=O distances are 1.240(3) and 1.236(5) Å, while those in the ester group are 1.216(3) and 1.217(4) Å, which resemble typical carbonyl groups in their mononuclear analogues.<sup>25</sup> Weak hydrogen bonds are observed in complexes **1**·MeOH and **4** (Table S2, detailed description in the Supporting Information).

**Table 1.** Selected Bond Lengths (Å) and Bond Angles (°) for **1**·MeOH and **4**.

<b>1</b> ·MeOH		<b>4</b>	
Pt1–O1	1.9857(18)	Pt1–O1	1.969(3)
Pt1–N1	2.030(2)	Pt1–N1	2.030(3)
Pt1–N7	2.038(2)	Pt1–N7	2.033(3)
Pt1–O13	2.0185(18)	Pt1–O13	2.059(3)
Pt1–N20	2.053(2)	Pt1–N21	2.048(4)
Pt1–N23	2.052(2)	Pt1–N24	2.052(3)
N20–N21	1.211(3)	N21–N22	1.183(5)
N21–N22	1.140(4)	N22–N23	1.163(6)
N23–N24	1.220(3)	N24–N25	1.217(5)
N24–N25	1.138(4)	N25–N26	1.137(5)
O1–Pt1–O13	174.49(7)	O1–Pt1–O13	170.35(11)
N21–N20–Pt1	114.52(18)	N22–N21–Pt1	114.3(3)
N22–N21–N20	175.0(3)	N23–N22–N21	175.6(5)
N24–N23–Pt1	113.68(18)	N25–N24–Pt1	120.4(3)
N25–N24–N23	175.6(3)	N26–N25–N24	174.4(4)

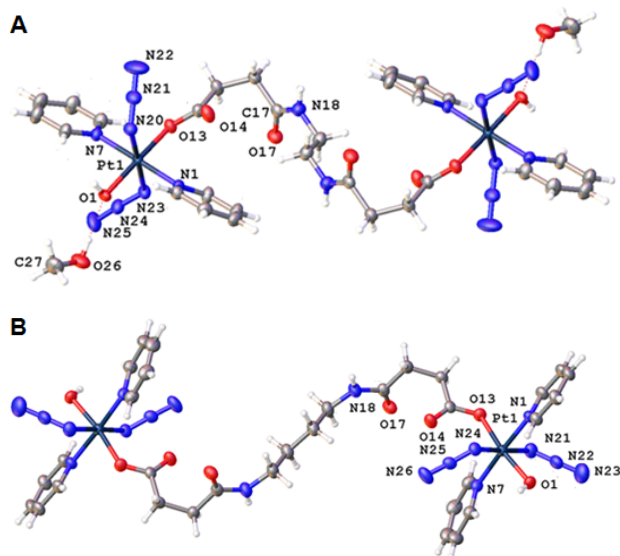


**Figure 1.** X-ray crystal structures of **1**·2MeOH (A) and **4** (B). The complexes sit on inversion centers and only the asymmetric unit is labelled. Thermal ellipsoids are drawn at the 50% probability level.

Compared with the fully symmetrical complex *trans, trans, trans*-[Pt(N<sub>3</sub>)<sub>2</sub>(OH)<sub>2</sub>(py)<sub>2</sub>], complexes **1**·2MeOH and **4** exhibit distortions from ideal octahedral geometry. The axial bond angles between  $Pt^{IV}$  and *trans* donor atoms are  $<180^\circ$  and the Pt–O (hydroxide, 1.9857(18) Å) bond is slightly shorter than Pt–O (succinate, 2.0185(18) Å), which can be attributed to the steric hindrance caused by the relatively bulky carboxylate groups. The azido ligands are almost linear with the Pt–N( $\alpha$ )–N( $\beta$ ) angles slightly smaller than  $120^\circ$ . The terminal azide N–N bond (1.140(4) and 1.138(4) Å) is slightly shorter than the azide N–N bond (1.211(3) and 1.220(3) Å) closest to Pt, which is typical of azide ligands due to their resonance structure. The Pt–N(pyridine) bond (2.030(2) and 2.038(2) Å) is shorter than the Pt–N(azide) bond

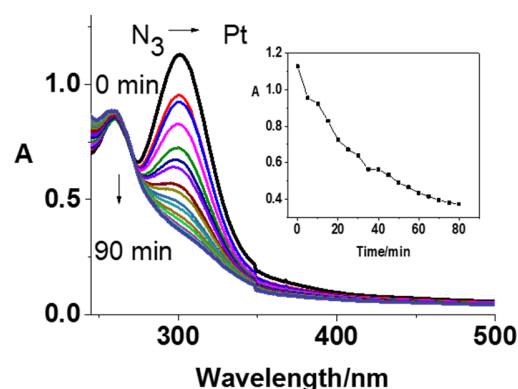


**Figure 2.** Photochemical decomposition with blue light (420 nm) of **1** ( $5 \times 10^{-5}$  M, in H<sub>2</sub>O: methanol 1:2 v/v) determined by UV-vis spectroscopy (Insert: time dependence of absorbance change at 300 nm).

**Photoactivation.** The photodecomposition of complexes **1–4** in aqueous solution was monitored by UV-vis spectroscopy at various

time intervals after irradiation with blue light (420 nm) at ambient temperature. Figure 2 shows the decrease in absorbance maximum of complex **1** at *ca.* 300 nm, assigned as the  $N_3 \rightarrow Pt$  LMCT band. The decrease indicates the release of the azide ligands was complete within 1 h. This photodecomposition behaviour is similar to that of the mono-Pt counterpart. Similar results were obtained for the other three complexes (Figure S9). Photoreactions of dinuclear complex **4** were investigated by LC-MS (Figure S10 and Table S3). The HPLC peak assigned to complex **4** disappeared within 10 min of irradiation with blue light (420 nm). Peaks assignable to dinuclear photoproducts increased in intensity gradually and peaked after 5 min, and then decreased over 30 min with a concomitant increase in the formation of mononuclear photoproducts  $[\{Pt^{II}(py)_2(OC(O)H)_2\}+Na]^+$  (466.05) and  $\{Pt^{II}(CH_3CN)(N_3)(py)_2\}^+$  (436.10). It appears that complex **4** loses one azide from both platinum centers initially, followed by the dissociation of a platinum center and the associated bridging ligand (Figure S10).

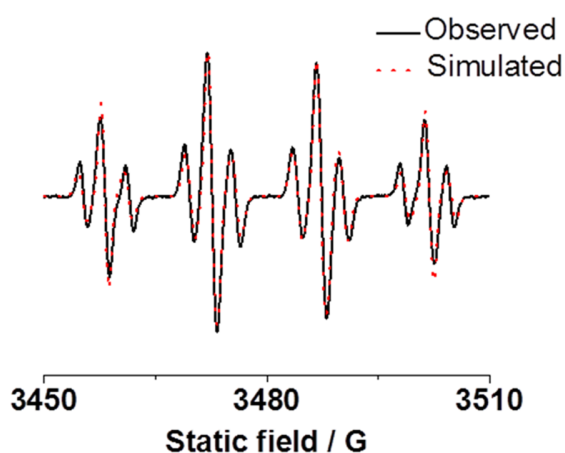


**Figure 3.** Observed (black) and simulated (red) EPR spectra of complex **4** in aqueous solution with 5% DMSO showing the formation of  $DMPO-N_3\cdot$  and  $DMPO-OH\cdot$  adducts after irradiation (465 nm). The experimental trace is the accumulation of 500 scans (conversion time 5.12 ms, time constant 5.12 ms, sweep time 10.48 s for each scan) with continuous irradiation (465 nm). Parameters for simulation:  $DMPO-N_3\cdot$  ( $g = 2.00583$ ,  $a_{NO}^N = 14.5$  mT,  $a_{\beta}^H = 14.2$  mT,  $a_{N\alpha}^N = 0.31$  mT);  $DMPO-OH\cdot$  ( $g = 2.0058$ ,  $a_{NO}^N = 14.5$  mT,  $a_{\beta}^H = 14.2$  mT).

**Formation of azidyl radicals.** The formation of azidyl radicals from the photodecomposition of these  $Pt^{IV}$  complexes was monitored by EPR using DMPO as a spin trap. EPR spectra were recorded continuously for 5 mM solution of complex **4** and 40 mM DMPO in 5% DMSO/95%  $H_2O$  on irradiation with blue light (465 nm, 20 mW) at 298 K. Both azidyl and hydroxyl radical adducts of DMPO ( $DMPO-N_3\cdot$  and  $DMPO-OH\cdot$ ) were detected upon irradiation, as a 1 : 2 : 2 : 1 quartet of triplets and a 1 : 2 : 2 : 1 quartet, respectively (Figure 3). The simulation was carried out using the parameters listed in Figure 3, which is in accordance with reference.<sup>23</sup>

**Photocytotoxicity and cellular accumulation studies.** Upon irradiation with blue light (465 nm, 4.8 mW/cm<sup>2</sup>, 1 h), complexes **1–4** exhibited photocytotoxicity towards several human cancer cell lines, including A2780, A2780cis ovarian and OE19 oesophageal cancer cells. The dose-dependent inhibition of cell viability determined by the sulforhodamine B (SRB) colorimetric assay both

in the dark and after irradiation of complexes **1–4**, is summarised in Table 2. In parental (A2780) and cisplatin resistant (A2780cis) ovarian carcinoma, complexes **1–4** showed no cytotoxicity in the dark. However, upon irradiation for 1 h, complexes **1–4** exhibited cytotoxicity to varying extents. Complex **4** was the most potent member of the series ( $IC_{50} = ca.$  17.0  $\mu M$  for ovarian cancer cells A2780 and A2780cis, and 8.8  $\mu M$  for OE19) with photocytotoxic index (PI) towards cancer cells > 6 for ovarian carcinoma and 11 for oesophageal adenocarcinoma with light exposure. Complexes **1** and **3** had lower  $IC_{50}$  values toward the cisplatin-resistant A2780cis cell line ( $IC_{50} = 29.5$   $\mu M$  (**1**), 35.5  $\mu M$  (**3**)) compared to the parental A2780 cell line ( $IC_{50} = 77.0$   $\mu M$  (**1**), 78.3  $\mu M$  (**3**)), which suggests a different mechanism of action from cisplatin and the possibility of overcoming the resistance. In contrast, the mononuclear analogue **FM-190** was 10x more toxic to parental A2780 (1.4  $\mu M$ ) compared with cisplatin resistant A2780cis (14.5  $\mu M$ ) cells upon irradiation with UVA (365 nm).<sup>21</sup> Complexes **1–4** displayed cytotoxicity towards OE19 both in the dark and upon irradiation. However, irradiation improved the cytotoxicity slightly for complexes **1–3**, and considerably so for **4**, with a photocytotoxic index (PI) >11 ( $IC_{50} = 97.0$   $\mu M$  (dark), 8.8  $\mu M$  (light)).

In contrast to the photocytotoxicity observed towards cancer cell lines, complexes **1–4** were relatively non-toxic toward the normal cell line MRC5, with  $IC_{50}$  values >100  $\mu M$ , even after irradiation (Table 2). Since azidyl and hydroxyl radicals generated from platinum(IV) complexes with azides are key species involved in cell death,<sup>23</sup> their relative non-cytotoxicity towards MRC5 may be due to the lower basal ROS level of healthy cells, with higher radical levels being needed to cause cell death.<sup>41</sup> For comparison, cisplatin tested under the same conditions induced little cytotoxicity in all cell lines due to the short incubation time (1 h,  $IC_{50} >100$   $\mu M$  with or without light).

Cellular accumulation is related to the molecular structure as well as the lipophilic nature of the complex and often correlates with the antiproliferative activity of metalldrugs. The extent of cellular uptake of complexes **1–4** was investigated by treating cancer cell lines with  $IC_{50}$  concentrations for 1 h in the dark. The cell accumulation of Pt was then determined by ICP-MS. As shown in Table 3, complex **3** exhibited > 5x higher Pt accumulation than other complexes in all cell lines, attributable to its aromatic bridge linker and higher lipophilicity. For complexes with aliphatic linkers, **1** showed slight higher levels of Pt accumulation in all cancer cell lines compared with complexes **2** and **4**. It is notable that accumulation of Pt from complex **4** in cisplatin-resistant A2780cis ovarian cancer cells is 2x that for the parental A2780 cell line, even though complex **4** is equally toxic to both cell lines. These results appear to support the ability of the dinuclear complexes to overcome resistance to cisplatin.

**Cell cycle analysis.** The effect of complexes **3** and **4** in the presence of light on the progression of the cell cycle was studied. Cells were exposed to prodrugs at equipotent photocytotoxic  $IC_{50}$  concentrations for 1 h in the dark, then irradiated for 1 h (465 nm, 4.8 mW/cm<sup>2</sup>, 1 h). After 24 h recovery, cells were stained in the dark with propidium iodide in the presence of RNase then analysed by flow cytometry. The results are summarised in Table S4 and Figure 4.

In all cancer cell lines, the populations of cells in the stages of the cycle were not affected by the complexes in the dark, but changed dramatically upon irradiation. In OE19 oesophageal cancer cells, a reduction of cells in the G0/G1 phase was observed (*ca.* 45% to 29%), paralleled by an accumulation of cells in the G2/M phases (*ca.* 36% to 57%), suggesting that dinuclear complexes **3** and **4** inhibit progression from G2/M to G0/G1 upon irradiation.

**Table 2.** IC<sub>50</sub> values and photocytotoxic index (PI) for complexes **1–4** obtained after 1 h incubation, 1 h irradiation (465 nm) and 24 h recovery. CDDP (cisplatin) and CPZ (chlorpromazine) were used as references.

Cell		IC <sub>50</sub> (μM) <sup>a</sup>				CDDP	CPZ	FM-190
		1	2	3	4			
A2780	Dark	> 100	> 100	> 100	> 100	> 100	> 100	> 100
	Irrad	77.0 ± 2.9	33.9 ± 5.2	78.3 ± 6.8	16.7 ± 3.3	> 100	6.0 ± 0.3	7.1 ± 0.4
	PI	> 1.3	> 2.9	> 1.3	> 6.0	-	> 16.7	> 14.0
A2780cis	Dark	> 100	> 100	> 100	> 100	> 100	51.0 ± 0.2	
	Irrad	29.5 ± 11.0	67.6 ± 15.7	35.5 ± 3.4	17.0 ± 2.3	> 100	6.0 ± 0.3	
	PI	> 3.4	> 1.5	> 2.8	> 5.8	-	8.5	
OE19	Dark	41.3 ± 3.2	49.8 ± 1.5	53.4 ± 0.4	97.0 ± 5.7	> 100		
	Irrad	36.2 ± 2.4	27.5 ± 5.1	43.7 ± 1.9	8.8 ± 0.9	> 100		
	PI	1.1	1.8	1.2	11.0	-	-	
MRC5	Dark	> 100	> 100	> 100	> 100	> 100	> 100	> 100
	Irrad	> 100	> 100	> 100	> 100	> 100	> 50	> 100

<sup>a</sup> Data are from three independent experiments.

**Table 3.** Cell accumulation of Pt (ng/10<sup>6</sup> cells) in cancer cells after exposure to complexes **1–4** (equipotent IC<sub>50</sub> concentration, 1 h, in dark).

Complex	Platinum accumulation (ng/10 <sup>6</sup> cells)		
	A2780	A2780cis	OE19
<b>1</b>	24 ± 8*	17 ± 6*	13 ± 1*
<b>2</b>	10 ± 2*	11 ± 2**	12 ± 2**
<b>3</b>	101 ± 6*	56 ± 17*	51 ± 5***
<b>4</b>	8 ± 1*	17 ± 2*	8 ± 2*
<b>FM-190</b>	0.8 ± 0.2*		

<sup>a</sup> All data were determined from triplicate samples and their statistical significance evaluated by a two-tail t-test with unequal variances. \*p < 0.05, \*\*p < 0.01, \*\*\*p < 0.005.

Photoactivated complex **4** induced more significant changes in the cell cycle progression compared with **3** (two-tail t-test with unequal variances against control, Table S4), consistent with the higher photocytotoxicity of complex **4**. Similar changes in cell cycle populations were found for A2780 and A2780cis ovarian cancer cells (Figure 4). This is in contrast to cisplatin which arrests cells in S phase,<sup>42</sup> suggesting a different mechanism of action and a lack of cross-resistance between complexes **3** and **4** and cisplatin.

**Photoinduced reactions with 5'-guanosine monophosphate (5'-GMP).** Since the N7 site of the DNA base guanine is a preferred target for platinum amine anticancer complexes, photoreactions of complex **4** with 5'-guanosine monophosphate were investigated. The photoreactions were carried out by irradiating solutions of complex **4** (30 μM) in 5% methanol/95% water v/v in the presence of 5'-GMP (2, 4 or 8 mol equiv.) with blue light (420 nm) at 310 K and monitored by reverse-phase HPLC (Figure S11, Table S5). The photorelease of the bridging ligand [HOOC(CH<sub>2</sub>)<sub>2</sub>C(O)NH(CH<sub>2</sub>)<sub>4</sub>NHC(O)(CH<sub>2</sub>)<sub>2</sub>COOH+H]<sup>+</sup> (289.21) was confirmed by LC-MS and the amount released did not change significantly when the ratio of 5'-GMP/Pt was increased. The major photoproduct is assignable as {Pt<sup>II</sup>(CH<sub>3</sub>CN)(py)<sub>2</sub>(GMP-H)}<sup>+</sup> (756.09), which increased in proportion at higher 5'-GMP ratios. In addition, two small peaks ascribed to {Pt<sup>II</sup>(N<sub>3</sub>)(py)<sub>2</sub>(GMP)}<sup>+</sup> (757.95) and {Pt<sup>II</sup>(OC(O)H)(py)<sub>2</sub>(GMP)}<sup>+</sup> (761.91) were detected. {Pt<sup>II</sup>(OC(O)H)(py)<sub>2</sub>(GMP)}<sup>+</sup> was formed due to the addition of formic acid in mobile phase of LC-MS. Complex **4** reacted completely within 1 h of irradiation. The time dependence of the formation of photoproducts from the UV-vis spectra and LC-MS data is shown in Figure S12. Even though the

decomposition of complex **4** can be detected within only 1 min of irradiation, the apparent decrease of the absorbance of 5'-GMP and the formation of {Pt<sup>II</sup>(CH<sub>3</sub>CN)(py)<sub>2</sub>(GMP-H)}<sup>+</sup> (756.09) is observed only after 5 min of irradiation. No dinuclear photoproduct with 5'-GMP was detected, which suggests that the Pt centers do not react with 5'-GMP until they are detached from the bridging ligands. The results above agree well with those previously reported for the parent complex and its succinate derivative, suggesting that the two Pt<sup>IV</sup> centers have little effect on each other during the photoreactions with 5'-GMP.

**DNA binding studies in cell-free media.** To further explore the differences between mono- and di-nuclear complexes, and the effect of bridge linkers, the DNA binding ability of photoactivated dinuclear complexes **1** and **4** was investigated in comparison with mononuclear **FM-190**.

*Ct*-DNA was mixed with complexes in 10 mM NaClO<sub>4</sub> and immediately irradiated with blue visible light (λ<sub>max</sub> = 455 nm) for 1 h then kept at 310 K in the dark. Aliquots were removed at various time intervals and quickly filtered using a Sephadex G-50 column to remove free (unbound) Pt. The Pt content in these DNA samples was determined by AAS and the concentration of DNA was determined by UV-vis to give the kinetics of Pt binding to *ct*-DNA. The amount of Pt bound to DNA increased with time for all complexes. No significant difference was found between the investigated complexes (Figure 5A).

The DNA intercalator EtBr was used as a fluorescent probe to characterize perturbations induced in DNA by the adducts with Pt complexes. Modification of DNA by platinum complexes under irradiation conditions resulted in a decrease of EtBr fluorescence.



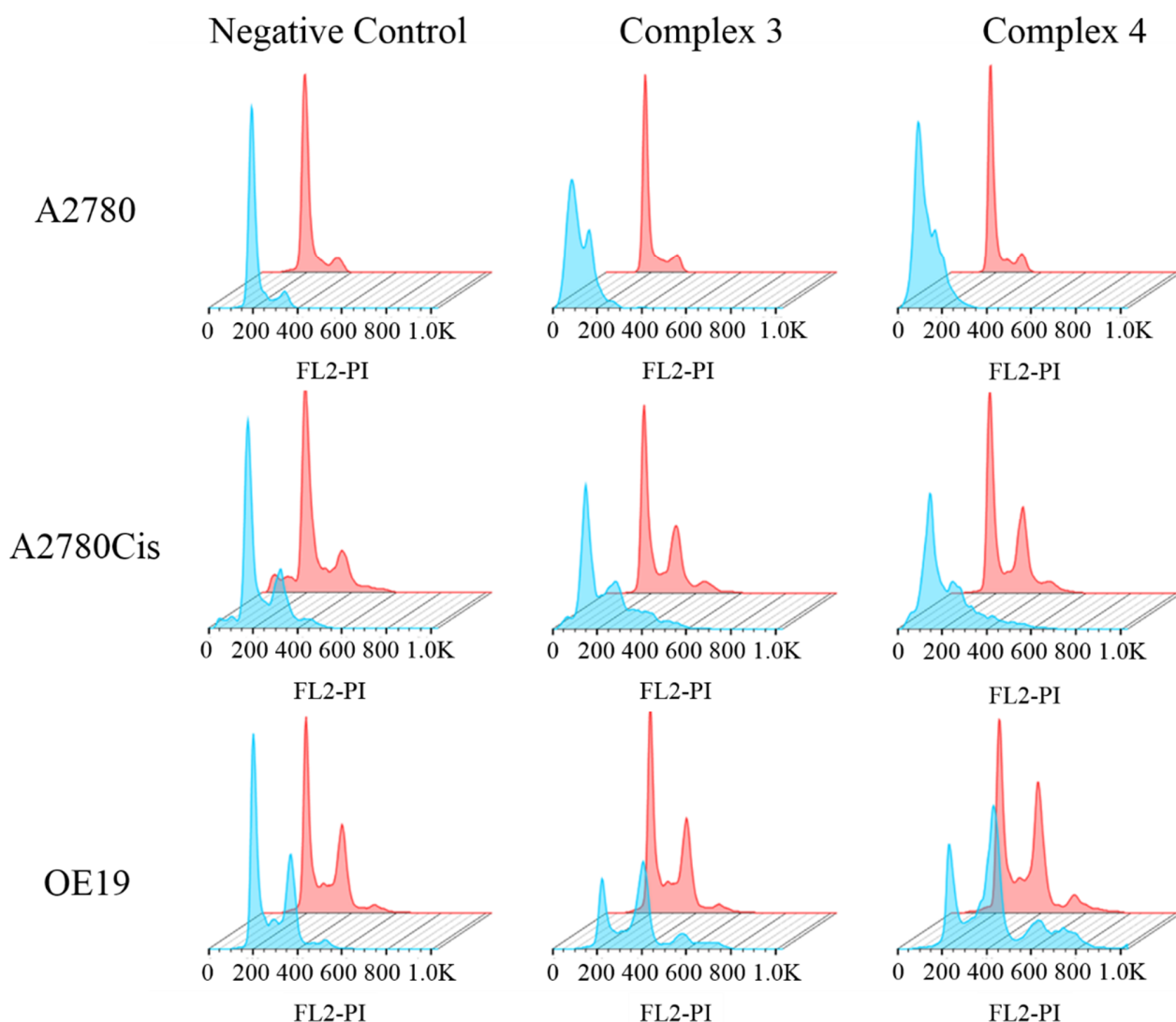


**Figure 4.** Flow cytometry histograms showing cell cycle analysis of A2780, A2780Cis ovarian and OE19 oesophageal cancer cells. (■ Dark, ■ Irradiated) In all cases, the experiments involved 1 h of drug exposure followed by 1 h of either irradiation (465 nm) or darkness. PI = Propidium Iodide.

The decrease caused by the adducts of photoactivated **1** or **4** was double than that induced by the DNA adducts of **FM-190** at equivalent  $\tau_b$  values (Figure 5B). It was also verified that irradiation of *ct*-DNA by visible light in the absence of complexes for 2 h had no effect on EtBr fluorescence. The results of these experiments suggest that the conformational distortions induced in DNA by the adducts formed by the treatment of DNA with irradiated **1** and **4** are delocalized and extend over the base pairs around the platination sites to an extent which corresponds to the distortions induced in DNA by two adducts of mononuclear **FM-190**. Thus, these results are consistent with the decomposition of the dinuclear complexes **1** and **4** due to irradiation resulting in the release of two mononuclear fragments similar to those from **FM-190**.

It was shown previously<sup>43</sup> that modification of DNA by irradiated **FM-190** resulted also the formation of DNA interstrand cross-links. Therefore, we investigated the capability of irradiated **1** and **4** to form DNA interstrand cross-links as well. Plasmid pUC19 linearized by EcoRI ( $50 \mu\text{g mL}^{-1}$ ) and the platinum complex were irradiated with blue light for 1 h and subsequently incubated in the dark for an additional 23 h in  $\text{NaClO}_4$  (10 mM) at 310 K. The

plasmid was modified to the extent corresponding to the  $\tau_b$  values of 0.003 and 0.0006 (in the case of **FM-190**) or 0.00015 and 0.0003 (in the case of **1** and **4**) and analyzed by agarose gel electrophoresis under denaturing conditions (Figure 5C). Interstrand crosslinked DNA appears as the top band (marked as ICLs) migrating on the gel more slowly than single-stranded DNA (contained in the bottom bands and marked as ss). The quantitative evaluation of the radioactivity associated with the individual bands showed that irradiated **1** and **4** formed two-fold amount of the interstrand crosslinks in DNA than **FM-190** (the frequency of interstrand crosslinking was  $12.5 \pm 0.5$ ,  $24 \pm 2$  and  $24 \pm 2$  for **FM-190**, **1** and **4**, respectively) at the same level of modification (related to the complex). Hence, the results of DNA interstrand cross-linking experiments also support the hypothesis that the irradiation of the dinuclear complexes **1** and **4** leads to their decomposition resulting in the release of two molecules similar to the photoproduct from mononuclear **FM-190**. Our previous work suggested that the *trans*- $\{\text{Pt}(\text{py})_2\}^{2+}$  fragment released from **FM-190** can form GG interstrand DNA cross-links, including 5'-CG/5'-CG cross-links, 5'-GC/5'-GC cross-links and cross-links between G and the

complementary C.<sup>44</sup> It is, therefore, reasonable to envisage that treatment of DNA by irradiated dinuclear **1** or **4** results in the formation of *trans* GG interstrand DNA cross-links as in the case of the treatment with mononuclear **FM-190**.

It has been shown that the binding of various antitumor metallodrugs to closed circular DNA can cause partial unfolding of the DNA. This process lowers the superhelical density of plasmid DNA, which causes a decrease in the rate of migration through an agarose gel. This fact makes it possible to observe and quantify the mean value of unwinding per adduct. In the present study, we investigated the unwinding induced in negatively supercoiled pSP73KB plasmid by **1**, **4** photoactivated by visible light ( $\lambda = 420$  nm) for 1 h, then incubated for another 23 h at 310 K in the dark. The degree of supercoiling was monitored using electrophoresis in a native agarose gel. We investigated the effect of increasing amounts of the investigated platinum complexes photoactivated by visible light bound to a mixture of relaxed and supercoiled pSP73KB DNA on migration of these forms in a native agarose gel (shown in Figure 5D). The unwinding angle is given by  $\Phi = -18\sigma/r_b(c)$ , where  $\sigma$  is the superhelical density, and  $r_b(c)$  is the value of  $r_b$  (related to the complex) at which the supercoiled and nicked forms comigrate. The DNA unwinding angle determined for DNA modified by dinuclear **1** and **4** photoactivated by visible light was  $57 \pm 8^\circ$ . This unwinding angle was two-fold higher than that found under identical conditions for DNA modified by mononuclear **FM-190** ( $28 \pm 4^\circ$ ).<sup>43</sup> Thus, consistent with the results of the experiments aimed at characterization of DNA adducts by EtBr fluorescence and DNA interstrand cross-linking, the results of DNA unwinding experiments (Figure 5D) can be interpreted to mean that the consequence of the irradiation of the dinuclear complexes **1** and **4** is their decomposition resulting in the release of two molecules of mononuclear **FM-190**.

A parameter which makes identification of preferential DNA binding sites of platinum antitumor drugs possible can be obtained from transcription mapping experiments.<sup>45</sup> *In vitro* RNA synthesis by RNA polymerases on DNA templates containing several types of bifunctional adducts of platinum complexes can be prematurely terminated at the level, or in the proximity, of DNA adducts. We prepared a 212-bp fragment by cutting of pSP73KB DNA by NdeI and HpaI restriction endonucleases. A substantial part of its nucleotide sequence is shown in Figure S13B. This fragment contained a T7 RNA polymerase promoter (in the upper strand close to its 3'-end, Figure S13B). The experiments were carried out using this linear DNA fragment, modified by cisplatin, transplatin (in the dark), or **1** or **4** photoactivated by visible light. The samples were irradiated for 1 h and subsequently incubated in the dark for additional 23 h. The  $r_b$  values were in the range of 0.004 - 0.01 and are indicated in the legend to Figure S13A. The major stop signals for DNA modified by dinuclear **1** and **4** (Figure S13) were identical to those found previously under identical conditions for DNA modified by irradiated **FM-190**.<sup>43</sup>

In order to obtain further information on the sequence-specificity of DNA binding in dinuclear **1** and **4** analogues of complex **FM-190**, a DNase I footprinting experiment was also performed (Figure S14). The details of this experiment are described in the Supporting information. The results show that the preferential binding sites of dinuclear **1** and **4** are those containing mainly G/A-rich sequences and are identical to those of mononuclear **FM-190**. Collectively, the results of transcription mapping and DNase I footprinting experiments suggest that preferential DNA binding sites of irradiated dinuclear **1** and **4** are similar to those of mononuclear **FM-190** thus also supporting the hypothesis that the irradiation of the dinuclear complexes **1** and **4** results in their decomposition resulting in the release of two molecules similar to photoproducts from mononuclear **FM-190**.

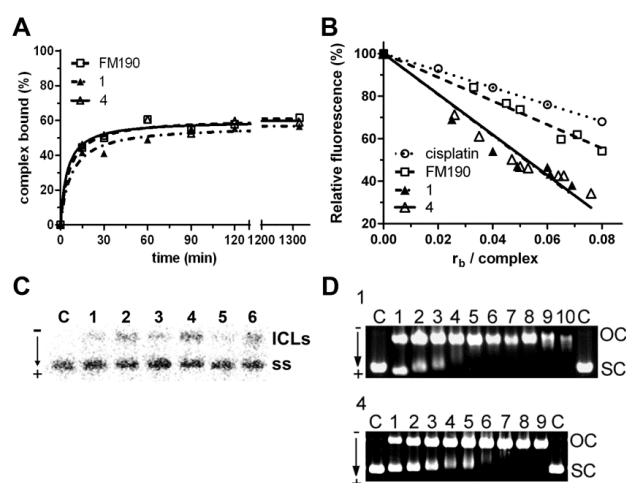


**Figure 5.** DNA binding of photoactivated complexes in cell-free media. A) Kinetics of the reaction of the investigated complexes photoactivated by visible light ( $\lambda_{\max} = 455$  nm) with *ct*DNA. For other details, see the text. B) Dependence of ethidium bromide fluorescence on  $r_b$  for double-helical *ct*DNA modified by the investigated platinum complexes photoactivated by visible light ( $\lambda_{\max} = 455$  nm) in NaClO<sub>4</sub> (10 mM) at 37 °C for 24 h. C) Formation of interstrand (intramolecular) cross-links by the investigated platinum complexes photoactivated by visible light ( $\lambda_{\max} = 455$  nm) in pUC19 plasmid linearized by EcoRI. Solutions of the linearized plasmid (50  $\mu\text{g mL}^{-1}$ ) were incubated with the platinum complex under irradiation conditions (for 1 h and subsequently incubated in the dark for an additional 23 h) at various  $r_b$  values in NaClO<sub>4</sub> (10 mM) at 37 °C. Autoradiogram of denaturing 1% agarose gel of linearized DNA which was 3'-end labeled and nonmodified and nonirradiated (kept in the dark) (lane C) or modified by photoactivated **FM-190** ( $r_b = 0.0003$  and 0.0006, lanes 1, 2, respectively), **1** ( $r_b = 0.00015$  and 0.0003, lanes 3, 4, respectively), or **4** ( $r_b = 0.00015$  and 0.0003, lanes 5, 6, respectively). Interstrand crosslinked DNA appears as the top bands (marked as ICL) migrating on the gel more slowly than single-stranded DNA (contained in the bottom bands and marked as ss). D) Unwinding of supercoiled pSP73KB plasmid DNA by the investigated dinuclear platinum complexes photoactivated by visible light ( $\lambda_{\max} = 455$  nm). The top bands correspond to the nicked form of the plasmid and the bottom bands to the closed, negatively supercoiled plasmid. The plasmid was incubated with **FM-190**, **1** and **4** under irradiation conditions (for 1 h and subsequently incubated in the dark for an additional 23 h) at various  $r_b$  values in NaClO<sub>4</sub> (10 mM) at 37 °C. Lane C, control, nonplatinated and nonirradiated DNA ( $r_b = 0$ ); lanes 1–10, DNA modified by photoactivated complexes so that the resulting  $r_b$  values were: for **FM-190**: 0.001, 0.003, 0.005, 0.010, 0.015, 0.020, 0.025, 0.030, 0.035 and 0.040 respectively; for **1**: 0.0005, 0.0025, 0.005, 0.0075, 0.01, 0.0125, 0.015, 0.0175, 0.02 and 0.025 respectively; for **4**: 0.001, 0.0015, 0.0025, 0.0035, 0.005, 0.01, 0.015, 0.0175 and 0.02 respectively.

## CONCLUSIONS

We report the synthesis and characterization of a series of novel dinuclear photoactive platinum(IV) anticancer prodrugs *trans*, *trans*, *trans*-[Pt(N<sub>3</sub>)<sub>2</sub>(py)<sub>2</sub>(OH)(OC(O)CH<sub>2</sub>CH<sub>2</sub>C(O)NH)<sub>2</sub>R] containing pyridine (py) and bridging dicarboxylate (R = -CH<sub>2</sub>CH<sub>2</sub>- (**1**); *trans*-1,2-C<sub>6</sub>H<sub>10</sub>- (**2**); *p*-C<sub>6</sub>H<sub>4</sub>- (**3**); -CH<sub>2</sub>CH<sub>2</sub>CH<sub>2</sub>CH<sub>2</sub>- (**4**)) ligands. We compared their photoreactivity with that of a mononuclear analogue **FM-190**. Azidyl and hydroxyl radicals and Pt<sup>II</sup> species were generated during the photodecomposition of these dinuclear complexes. LC-MS

analyses of photoreactions of dinuclear complex **4** revealed the photorelease of the bridging ligand and formation of mononuclear photoproducts. In the presence of 5'-GMP, the Pt<sup>II</sup>-5'-GMP adduct {Pt<sup>II</sup>(CH<sub>3</sub>CN)(py)<sub>2</sub>(GMP-H)}<sup>+</sup> (756.09) was formed upon irradiation. Dinuclear complexes exhibited promising photocytotoxicity upon irradiation with low-dose blue light (465 nm, 4.8 mW/cm<sup>2</sup>, 1 h, 1 h) towards a series of human cancer cell lines, including A2780, A2780cis, and OE19, with high dark stability. Moreover, the dinuclear complexes were remarkably non-toxic towards normal cells (MRC5), even after irradiation. The introduction of an aromatic bridging ligand enhanced cell uptake significantly for complex **3** when compared with the complexes containing an aliphatic bridge. The inhibition of progression from G2/M to G0/G1 stages in the cell cycle induced by dinuclear complexes upon irradiation suggests that DNA is a target. The dinuclear complexes behaved in cell-free media and after photoactivation similarly to the photoactivated mononuclear complex **FM-190** in terms of the kinetics of binding to *ct*-DNA, transcription mapping and DNase I footprinting of Pt-DNA adducts. However, dinuclear complexes after photoactivation were approximately two-fold more effective in quenching fluorescence of EtBr bound to DNA, forming DNA interstrand cross-links and unwinding DNA compared to photoactivated mono=Pt analogue **FM-190**. This is consistent with photodecomposition of the dinuclear complexes into two molecules of mononuclear platinum(II) species.

Hence, dinuclear complexes exhibit promising dark stability, photocytotoxicity and selectivity towards cancer cells, dependent on the nature of the bridging ligand.

## ASSOCIATED CONTENT

### Supporting Information

The Supporting Information is available free of charge on the ACS Publications website at DOI: 10.1021/acs.inorgchem.\*\*\*\*\*.

<sup>1</sup>H NMR, <sup>13</sup>C NMR spectra for all dinuclear complexes and UV-vis spectra (PDF). X-ray crystallographic files in CIF format for complexes **1** and **4**. Reactions with 5'-GMP, DNA binding and transcription mapping.

## AUTHOR INFORMATION

### Corresponding Author

\* Peter J. Sadler: [P.J.Sadler@warwick.ac.uk](mailto:P.J.Sadler@warwick.ac.uk)

### ORCID

Huayun Shi: 0000-0003-2334-7886

Isolda Romero-Canelón: 0000-0003-3847-4626

Monika Hreusova: 0000-0002-0888-7115

Olga Novakova: 0000-0003-2700-1284

V. Venkatesh: 0000-0001-9520-6842

Abraha Habtemariam: 0000-0003-2128-800X

Guy J. Clarkson: 0000-0003-3076-3191

Ji-inn Song: 0000-0002-0180-6423

Viktor Brabec: 0000-0002-8233-1393

Peter J. Sadler: 0000-0001-9160-1941

### Author Contributions

The manuscript was written through contributions of all authors. All authors have given approval to the final version of the manuscript.

### Notes

The authors declare no competing financial interest.

## ACKNOWLEDGEMENTS

This research was supported by the EPSRC (grants EP/G006792, EP/F034210/1 to PJS), ERC (grant 247450 to PJS), a Chancellor's International PhD Scholarship from the University of Warwick (for HS), the Czech Science Foundation (grant 18-09502S to ON and VB), Palacky University in Olomouc (IGAPrF2018 022 for MH), and the Royal Society (Newton International Fellowship and follow on funding AL170006\1 for VV).

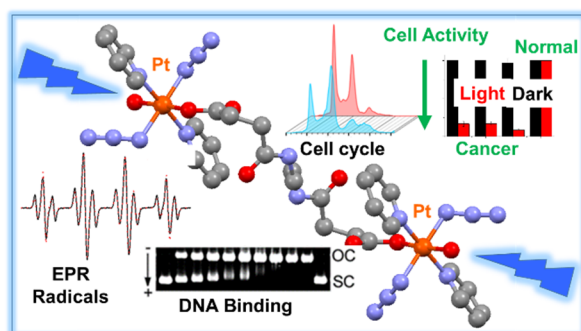
## REFERENCES

- Dolmans, D. E.; Fukumura, D.; Jain, R. K. Photodynamic therapy for cancer. *Nat. Rev. Cancer.* **2003**, *3*, 380–387.
- Bednarski, P. J.; Mackay, F. S.; Sadler, P. J. Photoactivatable platinum complexes. *AntiCancer Agents Med. Chem.* **2007**, *7*, 75–93.
- Bonnet, S. Why develop photoactivated chemotherapy? *Dalton Trans.* **2018**, 10.1039/c8dt01585f.
- Bjelosevica, A.; Pagesa, B. J.; Sparea, L. K.; Deoa, K. M.; Ang, D. L.; Aldrich-Wright, J. R. Exposing "Bright" metals: promising advances in photoactivated anticancer transition metal complexes. *Curr. Med. Chem.* **2018**, *25*, 478–492.
- Wong, E.; Giandomenico, C. M. Current status of platinum-based antitumor drugs. *Chem. Rev.* **1999**, *99*, 2451–2466.
- Pages, B. J.; Ang, D. L.; Wright, E. P.; Aldrich-Wright, J. R. Metal complex interactions with DNA. *Dalton Trans.* **2015**, *44*, 3505–3526.
- Harris, A. L. Hypoxia—a key regulatory factor in tumour growth. *Nat. Rev. Cancer.* **2002**, *2*, 38–47.
- Macquet, J. P.; Butour, J. L. Platinum-amine compounds: importance of the labile and inert ligands for their pharmacological activities toward L1210 leukemia cells. *J. Nat. Cancer Inst.* **1983**, *70*, 899–905.
- Van der Veer, J. L.; Peters, A. R.; Reedijk, J. Reaction products from platinum(IV) amine compounds and 5'-GMP are mainly bis(5'-GMP) platinum (II) amine adducts. *J. Inorg. Biochem.* **1986**, *26*, 137–142.
- Roat, R. M.; Reedijk, J. Reaction of mer-trichloro (diethylenetriamine)platinum(IV) chloride, (*mer*-[Pt(dien)Cl<sub>3</sub>]Cl), with purine nucleosides and nucleotides results in formation of platinum(II) as well as platinum(IV) complexes. *J. Inorg. Biochem.* **1993**, *52*, 263–274.
- Mitra, K. Platinum complexes as light promoted anticancer agents: a redefined strategy for controlled activation. *Dalton Trans.* **2016**, *45*, 19157–19171.
- Johnstone, T. C.; Suntharalingam, K.; Lippard, S. J. The next generation of platinum drugs: targeted Pt(II) agents, nanoparticle delivery, and Pt(IV) prodrugs. *Chem. Rev.* **2016**, *116*, 3436–3486.
- Shushakov, A. A.; Pozdnyakov, I. P.; Grivin, V. P.; Plyusnin, V. F.; Vasilchenko, D. B.; Zadesenets, A. V.; Melnikov, A. A.; Chekalind, S. V.; Glebov, E. M. Primary photochemical processes for Pt(IV) diazido complexes prospective in photodynamic therapy of tumors. *Dalton Trans.* **2017**, *46*, 9440–9450.

14. Müller, P.; Schröder, B.; Parkinson, J. A.; Kratochwil, N. A.; Coxall, R. A.; Parkin, A.; Parsons, S.; Sadler, P. J. Nucleotide cross-linking induced by photoreactions of platinum(IV)-azide complexes. *Angew. Chem. Int. Ed.* **2003**, *42*, 335–339.
15. Mackay, F. S.; Woods, J. A.; Heringová, P.; Kašpárková, J.; Pizarro, A. M.; Moggach, S. A.; Parsons, S.; Brabec, V.; Sadler, P. J. A potent cytotoxic photoactivated platinum complex. *Proc. Natl. Acad. Sci. USA.* **2007**, *104*, 20743–20748.
16. Westendorf, A. F.; Zerzankova, L.; Salassa, L.; Sadler, P. J.; Brabec, V.; Bednarski, P. J. Influence of pyridine versus piperidine ligands on the chemical, DNA binding and cytotoxic properties of light activated *trans*, *trans*, *trans*-[Pt(N<sub>3</sub>)<sub>2</sub>(OH)<sub>2</sub>(NH<sub>3</sub>)(L)]. *J. Inorg. Biochem.* **2011**, *105*, 652–662.
17. Mackay, F. S.; Moggach, S. A.; Collins, A.; Parsons, S.; Sadler, P. J. Photoactive *trans* ammine/amine diazido platinum(IV) complexes. *Inorg. Chim. Acta.* **2009**, *362*, 811–819.
18. Zhao, Y.; Farrer, N. J.; Li, H.; Butler, J. S.; McQuitty, R. J.; Habtemariam, A.; Wang, F.; Sadler, P. J. De novo generation of singlet oxygen and ammine ligands by photoactivation of a platinum anticancer complex. *Angew. Chem. Int. Ed.* **2013**, *52*, 13633–13637.
19. Zhao, Y.; Woods, J. A.; Farrer, N. J.; Robinson, K. S.; Pracharova, J.; Kasparkova, J.; Novakova, O.; Li, H.; Salassa, L.; Pizarro, A. M.; Clarkson, G. J.; Song, L.; Brabec, V.; Sadler, P. J. Diazido mixed-amine platinum(IV) anticancer complexes activatable by visible-light form novel DNA adducts. *Chem. Eur. J.* **2013**, *19*, 9578–9591.
20. Kasparkova, J.; Kostrhunova, H.; Novakova, O.; Křikavová, R.; Vančo, J.; Trávníček, Z.; Brabec, V. A Photoactivatable platinum(IV) complex targeting genomic DNA and histone deacetylases. *Angew. Chem. Int. Ed.* **2015**, *54*, 14478–14482.
21. Farrer, N. J.; Woods, J. A.; Salassa, L.; Zhao, Y.; Robinson, K. S.; Clarkson, G.; Mackay, F. S.; Sadler, P. J. A potent trans-diimine platinum anticancer complex photoactivated by visible light. *Angew. Chem. Int. Ed.* **2010**, *49*, 8905–8908.
22. Pracharova, J.; Zerzankova, L.; Stepankova, J.; Novakova, O.; Farrer, N. J.; Sadler, P. J.; Brabec, V.; Kasparkova, Interactions of DNA with a new platinum(IV) azide dipyrindine complex activated by UVA and visible light: Relationship to toxicity in tumor cells. *J. Chem. Res. Toxicol.* **2012**, *25*, 1099–1111.
23. Butler, J. S.; Woods, J. A.; Farrer, N. J.; Newton, M. E.; Sadler, P. J. Tryptophan switch for a photoactivated platinum anticancer complex. *J. Am. Chem. Soc.* **2012**, *134*, 16508–16511.
24. Gandioso, A.; Shaili, E.; Massaguer, A.; Artigas, G.; González-Cantó, A.; Woods, J. A.; Sadler, P. J.; Marchán, V. An integrin-targeted photoactivatable Pt(IV) complex as a selective anticancer pro-drug: synthesis and photoactivation studies. *Chem. Commun.* **2015**, *51*, 9169–9172.
25. Shaili, E.; Fernández-Giménez, M.; Rodríguez-Astor, S.; Gandioso, A.; Sandín, L.; García-Vélez, C.; Massaguer, A.; Clarkson, G. J.; Woods, J. A.; Sadler, P. J.; Marchán, V. A photoactivatable platinum(IV) anticancer complex conjugated to the RNA ligand Guanidinoneomycin. *Chem. Eur. J.* **2015**, *21*, 18474–18486.
26. Venkatesh, V.; Wedge, C. J.; Romero-Canelón, I.; Habtemariam, A.; Sadler, P. J. Spin-labelled photo-cytotoxic diazido platinum(IV) anticancer complex. *Dalton Trans.* **2016**, *45*, 13034–13037.
27. Min, Y.; Li, J.; Liu, F.; Yeow, E. K. L.; Xing, B. Near-infrared light-mediated photoactivation of a platinum antitumor prodrug and simultaneous cellular apoptosis imaging by upconversion-luminescent nanoparticles. *Angew. Chem. Int. Ed.* **2014**, *53*, 1012–1016.
28. Venkatesh, V.; Mishra, N. K.; Romero-Canelón, I.; Vernooij, R. R.; Shi, H.; Coverdale, J. P. C.; Habtemariam, A.; Verma, S.; Sadler, P. J. Supramolecular photoactivatable anticancer hydrogels. *J. Am. Chem. Soc.* **2017**, *139*, 5656–5659.
29. Malina, J.; Farrell, N. P.; Brabec, V. DNA condensing effects and sequence selectivity of DNA binding of antitumor noncovalent polynuclear platinum complexes. *Inorg. Chem.* **2014**, *53*, 1662–1671.
30. Cox, J. W.; Berners-Price, S.; Davies, M. S.; Qu, Y.; Farrell, N. P. Kinetic analysis of the stepwise formation of a long-range DNA interstrand cross-link by a dinuclear platinum antitumor complex: evidence for aquated intermediates and formation of both kinetically and thermodynamically controlled conformers. *J. Am. Chem. Soc.* **2001**, *123*, 1316–1326.
31. Qu, Y.; Scarsdale, N. J.; Tran, M. C.; Farrell, N. P. Cooperative effects in long-range 1,4 DNA-DNA interstrand cross-links formed by polynuclear platinum complexes: an unexpected syn orientation of adenine bases outside the binding sites. *J. Biol. Inorg. Chem.* **2003**, *8*, 19–28.
32. Hegmans, A.; Berners-Price, S. J.; Davies, M. S.; Thomas, D.; Humphreys, A.; Farrell, N. P. Long range 1,4 and 1,6-interstrand cross-links formed by a trinuclear platinum complex. minor groove preassociation affects kinetics and mechanism of cross-link formation as well as adduct structure. *J. Am. Chem. Soc.* **2004**, *126*, 2166–2180.
33. Malina, J.; Farrell, N. P.; Brabec, V. DNA interstrand cross-links of an antitumor trinuclear platinum(II) complex: thermodynamic analysis and chemical probing. *Chem. Asian J.* **2011**, *6*, 1566–1574.
34. Gourley, C.; Cassidy, J.; Edwards, C.; Samuel, L.; Bisset, D.; Camboni, G.; Young, A.; Boyle, D.; Jodrell, D. A phase I study of the trinuclear platinum compound, BBR 3464, in combination with protracted venous infusional 5-fluorouracil in patients with advanced cancer. *Cancer Chemother. Pharmacol.* **2004**, *53*, 95–101.
35. Jodrell, D. I.; Evans, T. R. J.; Steward, W.; Cameron, D.; Prendiville, J.; Aschele, C.; Noberasco, C.; Lind, M.; Carmichael, J.; Dobbs, N.; Camboni, G.; Gatti, B.; Braud, F. D. Phase II studies of BBR3464, a novel tri-nuclear platinum complex, in patients with gastric or gastro-oesophageal adenocarcinoma. *Eur. J. Cancer.* **2004**, *40*, 1872–1877.
36. Hensing, T. A.; Hanna, N. H.; Gillenwater, H. H.; Camboni, M. G.; Allievi, C.; Socinski, M. A. Phase II study of BBR 3464 as treatment in patients with sensitive or refractory small cell lung cancer. *AntiCancer Drugs*, 2006, *17*, 697–704.
37. Dolomanov, O. V.; Bourhis, L. J.; Gildea, R. J.; Howard, J. A. K.; Puschmann, H. OLEX2: a complete structure solution, refinement and analysis program. *J. Appl. Cryst.* **2009**, *42*, 339–341.
38. Sheldrick, G. M. SHELXT-Integrated space-group and crystal-structure determination. *Acta Cryst.* **2015**, *A71*, 3–8.
39. Sheldrick, G. M. Crystal structure refinement with SHELXL. *Acta Cryst.* **2015**, *C71*, 3–8.
40. Vichai, V.; Kirtikara, K. Sulforhodamine B colorimetric assay for cytotoxicity screening. *Nat. Protoc.* **2006**, *1*, 1112–1116.
41. Halliwell, B. Oxidative stress and cancer: have we moved forward? *Biochem. J.* **2007**, *401*, 1–11.
42. Muhammad, N.; Sadia, N.; Zhu, C.; Luo, C.; Guo, Z.; Wang, X. Biotin-tagged platinum(IV) complexes as targeted

- cytostatic agents against breast cancer cells, *Chem. Commun.* **2017**, 53, 9971–9974.
43. Pracharova, J.; Zerzankova, L.; Stepankova, J.; Novakova, O.; Farrer, N. J.; Sadler, P. J.; Brabec, V.; Kasparkova, J. Interactions of DNA with a new platinum(IV) azide dipyridine complex activated by UVA and visible light: relationship to toxicity in tumor cells. *Chem. Res. Toxicol.* **2012**, 25, 1099–1111.
44. C.Tai, H.; Brodbeck, R.; Kasparkova, J.; Farrer, N. J.; Brabec, V.; Sadler, P. J.; Deeth, R. J. Combined theoretical and computational study of interstrand DNA guanine–guanine cross-linking by *trans*-[Pt(pyridine)<sub>2</sub>] derived from the photoactivated prodrug *trans, trans, trans*-[Pt(N<sub>3</sub>)<sub>2</sub>(OH)<sub>2</sub>(pyridine)<sub>2</sub>]. *Inorg. Chem.* **2012**, 51, 6830–6841.
45. Brabec, V.; Leng, M. DNA interstrand cross-links of trans-diamminedichloroplatinum(II) are preferentially formed between guanine and complementary cytosine residues. *Proc. Natl. Acad. Sci. USA.* **1993**, 90, 5345–534.

## TOC



## Synopsis

Novel *all-trans* dinuclear platinum(IV) complexes bridged by a dicarboxylate linker, highly stable in the dark, generate azidyl and hydroxyl radicals on irradiation with blue light. They are photocytotoxic to human cancer cells, whereas cisplatin was inactive under these conditions, and more photoactive towards cisplatin-resistant ovarian cancer cells compared to wild-type cells. Remarkably, the dinuclear complexes were relatively non-toxic toward normal human cells. Cell cycle and DNA binding experiments suggested that DNA is a target.